

A Machine Learning Approach for Artifact Removal from Brain Signal

Sandhyalati Behera and Mihir Narayan Mohanty*

Department of Electronics and Communication Engineering, ITER, Sikhsha 'O'Anusandhan (Deemed to be University),
Bhubaneswar, 751030, India

*Corresponding Author: Mihir Narayan Mohanty. Email: mihirmohanty@soa.ac.in

Received: 08 March 2022; Accepted: 27 May 2022

Abstract: Electroencephalography (EEG), helps to analyze the neuronal activity of a human brain in the form of electrical signals with high temporal resolution in the millisecond range. To extract clean clinical information from EEG signals, it is essential to remove unwanted artifacts that are due to different causes including at the time of acquisition. In this piece of work, the authors considered the EEG signal contaminated with Electrocardiogram (ECG) artifacts that occurs mostly in cardiac patients. The clean EEG is taken from the openly available Mendeley database whereas the ECG signal is collected from the Physionet database to create artifacts in the EEG signal and verify the proposed algorithm. Being the artifactual signal is non-linear and non-stationary the Random Vector Functional Link Network (RVFLN) model is used in this case. The Machine Learning approach has taken a leading role in every field of current research and RVFLN is one of them. For the proof of adaptive nature, the model is designed with EEG as a reference and artifactual EEG as input. The peaks of ECG signals are evaluated for artifact estimation as the amplitude is higher than the EEG signal. To vary the weight and reduce the error, an exponentially weighted Recursive Least Square (RLS) algorithm is used to design the adaptive filter with the novel RVFLN model. The random vectors are considered in this model with a radial basis function to satisfy the required signal experimentation. It is found that the result is excellent in terms of Mean Square Error (MSE), Normalized Mean Square Error (NMSE), Relative Error (RE), Gain in Signal to Artifact Ratio (GSAR), Signal Noise Ratio (SNR), Information Quantity (IQ), and Improvement in Normalized Power Spectrum (INPS). Also, the proposed method is compared with the earlier methods to show its efficacy.

Keywords: Random vector functional link network (RVFLN); information quantity (IQ); constrained independent component analysis (cICA)

1 Introduction

Electroencephalogram (EEG) is a non-invasive procedure of recording the neurophysiological activity of the brain signal by placing the electrodes over the scalp. Due to its non-invasiveness, the EEG signal is extensively used for the detection and prediction of neurological problems of the brain such as sleep



This work is licensed under a Creative Commons Attribution 4.0 International License, which permits unrestricted use, distribution, and reproduction in any medium, provided the original work is properly cited.

disorders, abnormalities in the brain (such as seizure, hypercapnia, and asphyxia), and monitoring alertness, coma, and brain death, etc. [1–5]. Therefore, the accurate analysis of EEG signals is extremely important in the field of neuro-clinical applications. The time at which the neurological activities of the brain are recorded at the same time the physiological and non-physiological artifacts become an integral part of it. Physiological artifacts are generated by the physiological activity of the body like eyelid movement, muscular contraction, body movement, and electrical activity of the heart. The movement of the eyelid creates ocular artifacts and these artifacts are mostly affected by lateral frontal electrodes [6]. Various algorithms are developed for the removal of ocular artifacts [7–14]. The ECG artifacts are mostly observed at mid-temporal and posterior temporal electrodes. The ECG artifacts are coincidental with the ECG tracing and synchronize with the combined Q wave, R Wave, and S Wave “QRS complex” of the ECG channel. Non-physiological artifacts are removed by taking appropriate caution however, physiological artifacts embedded with the EEG signal need separate artifact removal algorithms before analyzing to obtain clinical information. Various artifact removal techniques are developed by the researchers for the removal of the cardiac artifact. However, the research continues and become a challenge for the researchers to develop a robust model that can be used to remove artifact of different kinds with minimal loss of information.

In the proposed work, the authors have come up with one new technique which uses the RVFLN model for the removal of artifacts from the brain signal. In the RVFLN model, the weights between the input layer to the hidden layer are randomly chosen. Due to this, the original feature space is mapped into an unexpected feature space. The random feature mapping mechanism of RVFLN plays a vital role in the performance of RVFLN. The important characteristics of RVFLN such as simple architecture, fast training speed, and universal approximation capability. Since there is very little to explore in the RVFLN model and as the RVFLN model has not yet been used for artifact removal application which is similar to an adaptive filter is used in this approach. The neural network model acts as the adaptive filter. As the signal is mixed with the ECG artifacts, it becomes complex and non-stationary. To filter out the artifacts RVFLN is considered. It acts well as an adaptive filter for each time segment verification. The writing arrangement for the proposed work is as follows: Sections 1 and 2 are for Introduction and discussion about the related works, Section 3 is for Materials used and discussion about the techniques used, Section 4 is about results and discussion and the last section is about conclusion and references.

2 Related Work

For removal of interference from EEG signals various techniques were developed. Filtering techniques, Blind Source Separation (BSS) such as Independent Component Analysis (ICA), Principal Component Analysis (PCA), etc., and some hybrid techniques are already applied for the removal of EEG artifacts. The ICA was applied for the removal of ECG artifacts from EEG signals. In this case, the authors had considered EEG signals recorded from small animals and had neglected the differences between human and small animals' brain signals. Before the use of the ICA algorithm, the EEG signal passed through two pre-processing stages they were mean removal and signal whitening with the help of the whitening matrix. The separating matrix for ICA was found by maximizing the absolute value of kurtosis. Once the separation matrix was found, the row representing the ECG component in an independent component matrix was set to zero for the removal of the ECG artifact. For the performance measure, the author had taken INPS and found the value as 7.71 ± 3.63 dB initially and 1.15 ± 0.6 dB after 1 h of recovery [15]. The modification of ICA was done by the author in [16,17] applied for the removal of ECG artifacts. The modification was in the case of finding the separation matrix. The separation matrix was found by maximizing the joint entropy and it was found by the gradient ascent algorithm. The performance of the modified ICA algorithm was compared with ensemble average subtraction (EAS) and adaptive filtering algorithm. The artifact-free signal was obtained with a correction rate of 91.0%. However, if there is a slight difference between cardiac interference and ECG then there are small changes in the performance.

Another modification to the ICA is constrained ICA (cICA) was used for the removal of pulse-related artifacts (PRA) by the author in [18]. The constraint in ICA is considered in a model of the PRA and the PRA template was computed for each channel of the EEG signal. The Clustering Constrained ICA (ccICA) was also used for the removal of the Ballisto-cardiogram (BCG) artifact. The clustering technique applied for the Clustering Constrained ICA (CCICA) algorithm catches the time-varying features of the artifact and constraint ICA removes these BCG artifacts. However, this algorithm's performance depends on the cluster types and types of clustering algorithms chosen [19]. The ICA with the help of an adaptive thresholding-based QRS detection algorithm was used by the author in [20] provides average sensitivity of above 99%. The performance of the algorithm depends fully on the QRS detector taken. PCA with the help of an adaptive Optimal Basis Set (aOBS) was used for the removal of BCG artifacts [21]. However, the BSS methods are based on some assumptions, and in all the cases the assumptions do not hold good. To avoid the problem of ICA the researchers combine the ICA with filtering and wavelet transform methods for artifact removal purposes.

Some Hybrid methods that are the combination of two or more methods are also taken for the removal of cardiac artifacts. The ICA with wavelet transforms was used for the removal of cardiac artifacts. The soft thresholding was applied to the wavelet coefficients for de-noise purposes. The wavelet transform was applied in the case of data protection [22]. The ICA with the help of a classification algorithm was used to classify the independent components into cardiac and non-cardiac components. The cardiac components were further classified into actual cardiac-related components (CCs) and Non-cardiac related components (NCCs). The actual CCs were again classified to know whether they were electrically generated cardiac components (ECCs) or Pulse generated cardiac components (PCCS). In the end, the CCs, ECCs, and PCCs were removed and the signal reconstruction took place only by considering NCCs [23]. The combination of ICA and continuous wavelet transform (ICA-CWT) is used for the removal of electrocardiogram artifacts from EEG signal which considers both temporal and spatial characteristics of the artifact. In this, the PCA was used for whitening the signal before applying ICA. After applying ICA, the selected number of Independent Components (ICs) are taken for further analysis. The selection criteria were that the ICs, whose spatial distribution on the head was similar to that of the pre-computed template. The continuous wavelet transform was applied to the selected ICs to improve peak detection. The locations of the peaks were obtained and tested for periodicity and the periodic components are rejected [24]. However, the Discrete Wavelet Transform (DWT) and Continuous Wavelet Transform (CWT) denoising methods based on a certain threshold value and appropriate choice of the threshold value are extremely important to avoid the change of any information loss. The wavelet analysis represents the signal in terms of the mother wavelet. The mother wavelet is the local function, not the global one. So, the corresponding filters do not provide a non-linear shift between input and output.

The Event Synchronous Adaptive Noise Canceller (ES-ANC) was used for the removal of ECG artifacts from the EEG signals. This method emphasizes the detection of QRS complex from EEG with the help of an adaptive filter. The adaptive filter weights are adjusted with the help of the Normalized least mean square (NLMS) algorithm [25]. The ECG artifact increases the standard deviation considerably larger than the EEG signal. The adaptive filtering method represented in [26] uses the artifact templates, which are obtained from the onset parameter of the QRS complex of the ECG artifact. The artifact templates were updated and adapted by minimizing the mean square error. The Morphological filter (MF) used in [27] was able to eliminate ECG-related artifacts from EEG signals. The elimination criteria were fully dependent on the generation of the Structuring Element (SE). MF does two operations involving SE and source data i.e., erosion and dilation. As MF filters are nonlinear, it modifies the geometrical features of time-domain data. However, choosing appropriate SE is difficult. Removal of ECG artifacts method presented in [28] uses Recursive Least Square (RLS) Notch Filter. In this ECG artifacts were modeled using the instantaneous frequency of the cardiac cycle. ECG artifacts were adaptively estimated using an

RLS notch filter and subtracted from the contaminated EEG data. However, the appropriate calculation of the instantaneous frequency component is essential for the performance of the Notch filter. The energy interval histogram method proposed by authors in [29] had taken three characteristics of ECG artifacts such as lack of correlation with EEG, the spike-like property, and the periodicity property. They had not used any reference channel for ECG artifact generation. The Energy Interval Histogram (EIH) method was used for detection and the modification of ensemble average subtraction was used for the elimination of ECG artifacts. The Empirical Mode Decomposition (EMD) and its improved version were used for the detection and removal of ECG artifacts in [30].

An adaptive network that combines the advantages of the Neuro-Fuzzy system, called the Adaptive Neuro-Fuzzy Interference System (ANFIS) used for the removal of cardiac-related artifacts. To optimize the ANFIS parameters, PSO (Particle Swarm Optimization) with generalized bell (gbell) function was used. For the ANFIS model reference, an ECG signal was required with the contaminated EEG signal as the input data [31]. Another neural network algorithm was the Real-Time Recurrent Learning (RTRL) algorithm, used for the removal of cardiac-related artifacts. The adaptive filter in Adaptive Noise Cancellation (ANC) was replaced with RTAL. The RTAL learning algorithm is a backpropagation algorithm in which the weight space is computed by steepest descent [32]. This algorithm can able to remove the combination of ECG and EMG artifacts. The proposed work is on the neural network-based RVFLN model and is given in the following section.

3 Materials and Methods Used

3.1 Signal Model

The artifactual EEG signal can be represented as the combination of EEG signal and ECG artifacts. Both EEG signals are nonlinear and non-stationary.

Mathematically it can be written as

$$Y_{Aeeg} = S_{eeg} + N_{eeg} \quad (1)$$

where from the Eq. (1) Y_{Aeeg} is the artifactual EEG signal, S_{eeg} is the clean EEG signal and N_{eeg} is the noise added to the clean EEG signal. The noise in this case is the cardiac artifact that is to be eliminated. The EEG signal is modeled with the help of a non-linear radial basis function and mathematically written as

$$S_{eeg}(t) = \sum_{l=1}^L \beta_{l,t} \mathcal{F} \left(\sum_{k=1}^K \alpha_{k,l} x_k + b_{t,l} \right) + b_{h,t} \quad (2)$$

From Eq. (2) the function \mathcal{F} is the non-linear function of inputs to the RVFLN. L is the number of hidden nodes. β_l is the weight between l th hidden layer node and the output node. $\alpha_{k,l}$ is the weight of the l th hidden node and $b_{t,l}$ is the bias of the l th hidden node. The diagrammatic representation of the RVFLN model used for the removal of the artifact from the EEG signal is shown in Fig. 1. The input signal is provided through the input layer. The number of nodes in the input layer defines the no of samples of the input signal given at a time to the RVFLN network. The enhancement layer is the hidden layer.

3.2 Parameter Estimation by RVFLN

From Eq. (1) it is shown that model parameters are estimated through RVFLN neural network. Most of the conventional data-driven modeling techniques fail to provide good performance due to interference occurring in outliers. For the proposed work RVFLN is used to find out the optimum model co-efficient. The structure of the RVFLN network is similar to that of a single hidden layer feed-forward neural network (SLFN), but the problem in SLFN such as the sensitive setting of the learning rate, very slow convergence, and local minima are resolved with the help of RVFLN in which the hidden node

parameters are randomly assigned based on certain probability distributions. The RVFLN and its variants are basically committed to solving the regression problems [33].

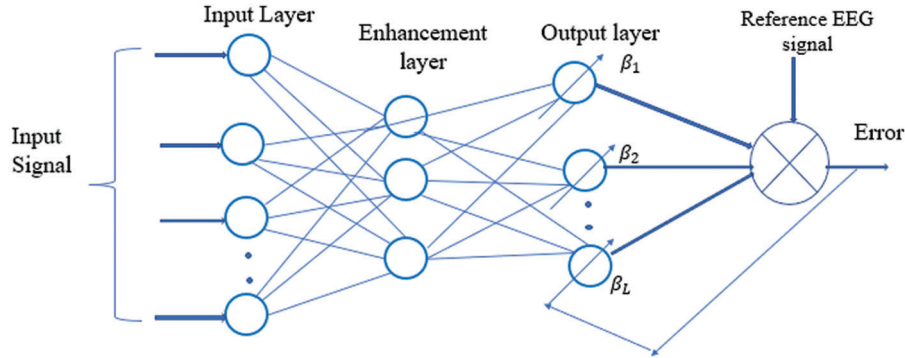


Figure 1: Diagrammatic representation of the proposed method

Similar to SLFN, RVFLN also has three layers as shown in Fig. 2. The three layers are the input layer, enhancement layer, and output layer. There is also some direct link between the input and output layers. These direct links help to regularize the enhancement features. The weights between the input and enhancement layer are randomly generated. These random weights transform the input features. After transforming the inputs, the activation function is applied to the transformed input to obtain the specific feature in the hidden layer. For the given set of training samples, the RVFLN for K hidden nodes is represented mathematically as

$$f(x) = \sum_{k=1}^K \beta_k h_k(\alpha_k, b_k, x) \tag{3}$$

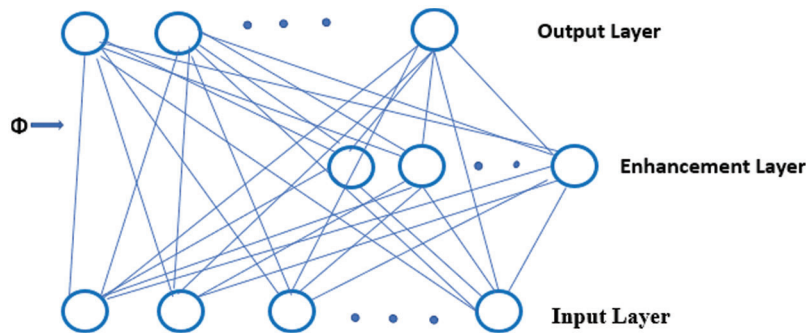


Figure 2: Structure of RVFLN

In the above Eq. (3) α_k and b_k represent the hidden layer parameters such as weight and bias respectively. β_k is the output weight between kth hidden layer node and the output node. h_k is the activation function for which radial basis function is generally used.

The activation function is given as

$$h_k = h\left(\frac{\|x - \alpha_k\|}{b_k}\right) \tag{4}$$

In the above equation $\|\cdot\|$ represents the l_2 norm. The parameters w_k and b_k are randomly assigned and the output layer parameters β_k needs to be estimated by the RVFNL network by minimizing the sum square error cost function which is written as

$$\psi = \sum_{i=1}^N \left\| \sum_{k=1}^K \beta_k h_k(w_k, b_k, x_i) - y_i \right\|^2 \quad (5)$$

The above equation is written in matrix form as

$$\psi = \operatorname{argmin}_{\beta} \|H\beta - Y\|^2 \quad (6)$$

From the Eq. (6) Y is the desired output and $\hat{Y} = H\beta$ is the estimated output. H is the hidden layer output as given in Eq. (7).

$$H = \begin{bmatrix} h(\alpha_1, b_1, x_1) & \cdots & h(\alpha_k, b_k, x_1) \\ \vdots & \ddots & \vdots \\ h(\alpha_1, b_1, x_N) & \cdots & h(\alpha_k, b_k, x_N) \end{bmatrix} \quad (7)$$

$$\beta = \begin{bmatrix} \beta_1 \\ \vdots \\ \beta_k \end{bmatrix} \quad \text{and} \quad Y = \begin{bmatrix} y_1 \\ \vdots \\ y_N \end{bmatrix} \quad (8)$$

The optimal output weight that minimizes the cost function ψ is obtained as

$$\beta = H^\dagger Y \quad (9)$$

H^\dagger is the pseudoinverse of $H = (H^T * H)^{-1} * H$.

The output weight is updated with the help of RLS algorithm which is given as follows:

$$\begin{aligned} \varepsilon(t) &= Y_{Aeeg} - \varphi^T(t) * \beta_i(t-1) \\ \beta_i(t) &= \beta_i(t-1) + k(t) * \varepsilon(t) \\ k(t) &= \frac{P(t-1)\varphi^T(t)}{\varphi^T(t)p(t-1)\varphi^T(t) + \lambda} \\ p(t) &= \frac{1}{\lambda} [p(t-1) - k(t)\varphi^T(t)p(t-1)] \end{aligned} \quad (10)$$

From the above algorithm λ is the forgetting parameter and is taken in between 0 and 1. $p(0) = \eta I$. I is the identity matrix and η is the large number taken as 10^4 . $\varphi(t)$ is the regression vector consists of taking past input and output samples. In special case it is considered as 1. $\varepsilon(t)$ is the error. Based on this error the output weights are updated.

3.3 Quantitative Measure

To evaluate the performances of ECG artifact removal method, the indicators taken are MSE, NMSE, RE, GSAR, SNR, IQ and INPS.

3.3.1 Mean Square Error (MSE)

The MSE is used as a measure of similarity between two signal. It measures the similarity between the clean EEG signal and the EEG signal obtained after the removal of artifact. Mathematically MSE is given by

$$MSE = \frac{1}{n} \sum_{i=1}^n (EEG_i - \widehat{EEG}_i)^2 \quad (11)$$

From Eq. (11) EEG_i is the clean EEG signal and \widehat{EEG}_i is the recovered EEG signal. The small value of MSE indicates the more similarity between two signal under consideration. Thus, the MSE is used as a degree of information preservation in EEG signal after removal of artifact.

3.3.2 Normalized Mean Square Error (NMSE)

The NMSE is also used as measure to evaluate the performance of artifact removal algorithm. The Normalized Mean Square Error is given by Eq. (12)

$$NMSE = \frac{\sum_{i=1}^N (EEG_i - \widehat{EEG}_i)^2}{N \sum_{i=1}^N EEG_i^2} \quad (12)$$

3.3.3 Relative Error (RE)

The Relative Error (RE) is a measure of precision. Mathematically the RE is calculated by Eq. (13)

$$RE = \frac{|\widehat{EEG}_i - EEG_i|}{EEG_i} \quad (13)$$

3.3.4 Gain in Signal to Artifact Ratio (Y)

The Gain in signal to artifact ratio is obtained after calculating Signal to Artifact Ratio (SAR) before and after the removal of artifact. The gain in signal to artifact ratio (Y) indicates wheather the signal to artifact ratio is improved or decreased or there is no improvement in signal quality. Mathematically the gain in signal to artifact ratio (Y) is given as:

$$Y = 10 \log_{10} \left(\frac{SAR_A}{SAR_B} \right) \quad (14)$$

In Eq. (14) SAR_A is the signal to artifact ratio after removal of artifact from the EEG signal and SAR_B is the signal to artifact ratio before artifact removal and are calculated by the using Eqs. (15) and (16) respectively.

$$SAR_A = \frac{\frac{1}{N} \sum_{i=1}^N |EEG_i|^2}{\frac{1}{N} \sum_{i=1}^N |\widehat{EEG}_i - EEG_i|^2} \quad (15)$$

$$SAR_B = \frac{\frac{1}{N} \sum_{i=1}^N |EEG_i|^2}{\frac{1}{N} \sum_{i=1}^N |EEG_{Con} - EEG_i|^2} \quad (16)$$

3.3.5 Signal to Noise Ratio (SNR)

The signal to noise ratio is given by

$$SNR = 10 \log_{10} \frac{EEG_i}{(\widehat{EEG}_i - EEG_i)} \quad (17)$$

The signal to noise ratio in Eq. (17) is expressed in dB. It is also used as a measure to evaluate the performance of artifact removal algorithm.

3.3.6 Information Quantity (IQ)

The IQ is used as a measure to validate the performance of the artifact removal algorithm as calculated in [34]. It is found by sliding temporal window technique and is given by Eq. (18)

$$W(n; w; \Delta) = \{EEG_i, i = 1 + n\Delta, \dots, w + n\Delta\} \quad (18)$$

where w is the sliding window and Δ is the sliding step $\Delta \leq w$. To find out IQ first DWT coefficients within each window are obtained as given in Eq. (19)

$$WDC(r; n; w; \Delta) = DWT[(W(n; w; \Delta))] \quad (19)$$

The probability in each transformed window is found out by introducing the interval I_m in that window which is given as

$$WDC(r; n; w; \Delta) = \cup_{m=1}^M I_m \quad (20)$$

The probability P_n is the signal sample belongs to the the interval I_m is the ratio of number of samples found within I_m and the total number of samples. The IQ is mathematically defined in Eq. (21) as

$$IQ(n) = - \sum_{m=1}^M P_n(m) \log_2(P_n(m)) \quad (21)$$

The high value of IQ indicates greater randomness in EEG signal i.e., more ECG artifact still present in EEG. Lower value of IQ indicates lower components of ECG artifact present in EEG signal. So, IQ is used as a measure of information preservation in EEG signal after removal of artifact.

3.3.7 INPS (Improvement in Normalized Power Spectrum)

INPS is used as a measure to evaluate the performance of the proposed algorithm. In this, the normalized power spectrum is calculated for the EEG signal before and after removal of artifact after passing EEG data through rectangular window using Welch method. Mathematically IMPS is given by the Eq. (22)

$$INPS = 10 \log_{10} \sum_{i=1}^N \frac{P_i^{EEG}}{\widehat{P_i^{EEG}}} \quad (22)$$

In Eq. (22) N is the number of harmonics considered. INPS indicates whearther the ECG artifact and their hamonics are effectively suppressed or not. Higher the value of INPS greater the performance of artifact removal algorithm.

4 Result and Discussion

In order to validate the performance of the proposed method the human brain signal is taken. The clean EEG signal is taken from the Mendeley data base [35]. The clean EEG signal is obtained from 14 males having mean age of 28.2 ± 7.5 and 13 females having mean age of 27.1 ± 5.2 . so total 17 set of clean EEG signal is available. Each set have 19 channels. The sampling frequency for this clean EEG signal is 200 Hz and each data set are of 30 sec durations. The artifact contaminated EEG signal is obtained by adding the cardiac interference with the clean simulated EEG signal. Mathematically,

$$Y_{Aeeg}(t) = S_{eeg}(t) + N_{eeg} = S_{eeg}(t) + c.e(t) \quad (23)$$

In the above Eq. (23) $e(t)$ is the cardiac interference which is generated by 10-fold filtering of the ECG signal and c is the scaling coefficient. By changing the scaling coefficient, the ECG interference is added to the signal with different noise ratio (SNR). The resultant artifactual EEG signal $x(t)$ is of 3600 sample sizes.

The clean EEG signal taken from the Mendeley data base have sample size 3600 as shown in Fig. 3. The clean EEG signal is taken as reference signal for the proposed algorithm. It is observed from the Fig. 3 that the amplitude of the clean EEG signal is within $4 \mu\text{V}$. The artifactual signal considered is shown in Fig. 4. The amplitude of the artifactual signal is more than the amplitude of the clean EEG signal.

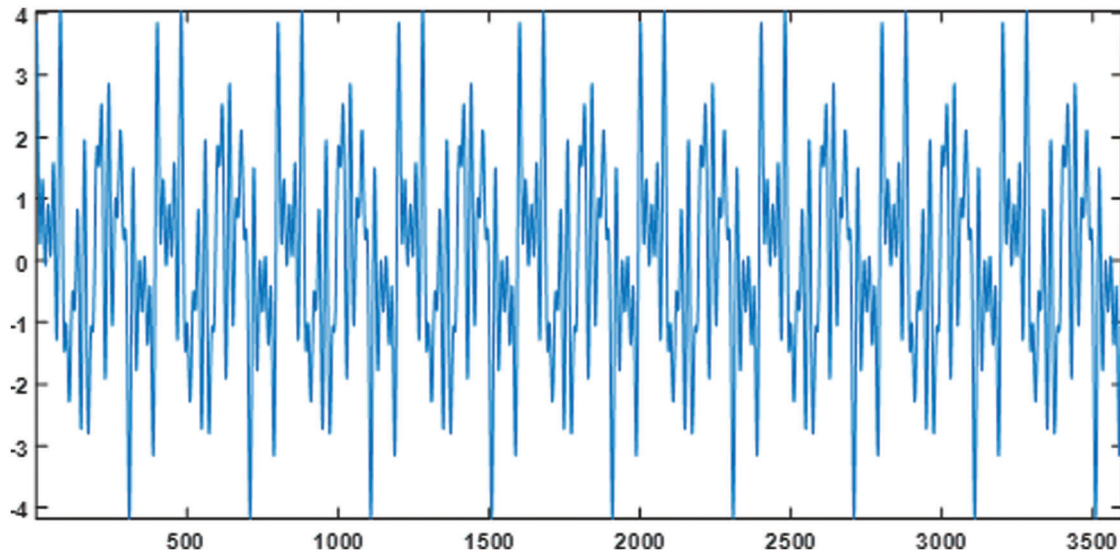


Figure 3: Clean EEG signal taken as reference

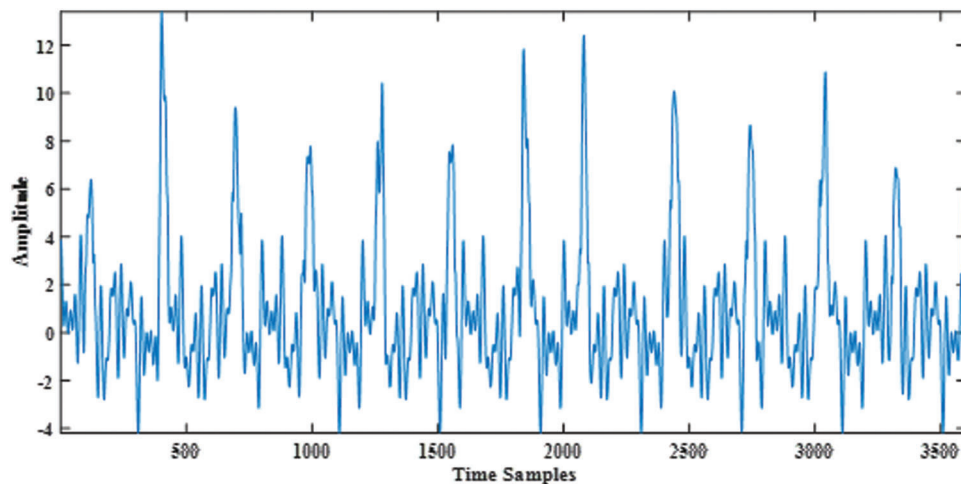


Figure 4: Artifactual EEG signal

Fig. 5 represents the recovered signal along with artifactual and clean signal. From Fig. 5, it can be observed well that the output of the proposed method ties with the desired signal. To validate the performance of the algorithm the quantitative measures are taken which are discussed in Section 3.3. The measurement parameters MSE and NMSE are in μV^2 . The Relative Error (RE) discussed above has no unit. The GSAR, SNR, IQ and INPS all in measured in dB. The MSE, NMSE and RE obtained are quite lesser. The SNR obtained for 0 dB SNR case is 68.4077 dB which indicates the signal is recovered without the loss of back ground information. The IQ obtained in the proposed algorithm is quite lesser

than the existing artifact removal algorithm which indicates more information is preserved after removal of artifact. The INPS obtained by the proposed algorithm is 9.95 dB.

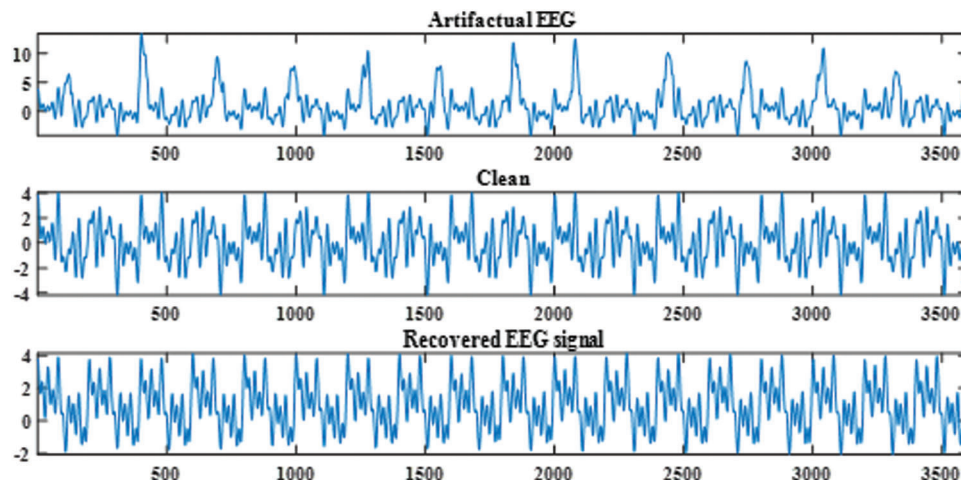


Figure 5: Artifactual EEG, Clean EEG and the Recovered EEG signal after denoising

The comparison of the proposed artifact removal algorithm is compared with some existing algorithm and is observed that the proposed algorithm performs well than the existing algorithm. The comparison table is shown in [Tab. 1](#).

Table 1: Comparison of performances with the existing algorithms

| Sl. No | Methods | MSE | NMSE | RE | GSAR | SNR | IQ |
|--------|-----------------------|-----------------------------|------------------|--------|------------|------------|-------|
| 1 | EMD + AF [30] | - | - | - | - | 51.4 dB | - |
| 2 | CEEMDAN + AF [30] | - | - | - | - | 53.5 dB | - |
| 3 | ANFIS + PSO [31] | $5.8904 \cdot 10^4 - 4 v^2$ | - | - | - | 21.8553 dB | - |
| 4 | Infomax | $3.31 \mu V^2$ | - | - | - | - | 0.341 |
| 5 | ICA | $5.59 \mu V^2$ | - | - | - | - | 0.350 |
| 6 | RLS notch filter [28] | $0.20 \mu V^2$ | - | - | - | - | 0.331 |
| 7 | Proposed Algorithm | $0.1998 \mu V^2$ | $0.4470 \mu V^2$ | 0.2771 | 10.4807 dB | 68.1117 dB | 0.330 |

As given in the [Tab. 1](#) the decomposition method EMD and adaptive filter used in [30] gives poor SNR than the proposed method. The EMD methods have many drawbacks such as end effect, mode-mixing. The Ensemble Empirical mode decomposition (EEMD) improves the performance of EMD by adding the White Gaussian noise. As a result, this white noise has not been completely offset after multiple averaging. The Complete Ensemble Empirical mode decomposition with Adaptive Noise (CEEMDAN) is the improved version of EEMD. So, the CEEMDAN provides better result than EEMD and adaptive filtering. The ICA algorithm assumes the resultant signal is the linear combination of sources and the sources are assumed

to be Gaussian but practically it is not possible in all the cases. The ICA and Infomax algorithms provide average result in the case of artifact removal from the EEG signal. The Recursive Least Square Notch filter method provides better result than ICA and Infomax and EMD with adaptive filter. In the case of RLS notch filter the exact frequency of the artifact needs to be known. The amplitude for each frequency component is estimated recursively with the help of Least Square algorithm. However, this method can also be unsuccessful when the exact frequency of the artifact component is unknown or difficult to calculate. The proposed methods overcome the demerits of the method under comparison and provides better result with minimal loss of information.

5 Conclusion

An RVFLN model was developed for removal Cardiac artifact from the EEG signal was successfully applied for EEG data without disturbing the background activity and the results found better than the existing methods because of the use of RVFLN which is used to estimate the exact parameter which are required for estimating the clean EEG signal from the artifactual EEG signal. The method can be applied for removal of other kinds of artifact also. Though this method is tested for ocular artifact and can be applied for other kinds of EEG dataset recorded in non-constrained environment.

Funding Statement: The authors received no specific funding for this study.

Conflicts of Interest: The authors declare that they have no conflicts of interest to report regarding the present study.

References

- [1] Y. Park, S. H. Han, W. Byun, J. H. Kim, H. C. Lee *et al.*, "A Real-time depth of anesthesia monitoring system based on deep neural network with large EDO tolerant EEG analog front-end," *IEEE Transactions on Biomedical Circuits and Systems*, vol. 14, no. 4, pp. 825–837, 2020.
- [2] J. Thomas, P. Thangavel, W. Y. Peh, J. Jing, R. Yuvaraj *et al.*, "Automated adult epilepsy diagnostic tool based on interictal scalp electroencephalogram characteristics: A six-center study," *International Journal of Neural Systems*, vol. 31, no. 5, pp. 2050074, 2021.
- [3] K. Rasheed, A. Qayyum, J. Qadir, S. Sivathamboo, P. Kwan *et al.*, "Machine learning for predicting epileptic seizures using EEG signals: A review," *IEEE Reviews in Biomedical Engineering*, vol. 14, pp. 139–155, 2020.
- [4] D. Kapgate, "Future of EEG based hybrid visual brain computer interface systems in rehabilitation of people with neurological disorders," *International Research Journal on Advanced Science Hub*, vol. 2, no. 6, pp. 15–20, 2020.
- [5] H. Raza, A. Chowdhury and S. Bhattacharyya, "Deep learning based prediction of EEG motor imagery of stroke patients' for neuro-rehabilitation application," in *2020 International Joint Conference on Neural Networks (IJCNN)*, Glasgow, UK, IEEE, pp. 1–8, 2020.
- [6] M. Sazgar and M. G. Young, "EEG artifacts," in *Absolute Epilepsy and EEG Rotation Review*, Springer, Cham, Switzerland, pp. 149–162, 2019.
- [7] M. Saini and U. Satija, "An effective and robust framework for ocular artifact removal from single-channel EEG signal based on variational mode decomposition," *IEEE Sensors Journal*, vol. 20, no. 1, pp. 369–376, 2019.
- [8] C. Zhang, Y. Lian and G. Wang, "ARDER: An automatic EEG artifacts detection and removal system," in *2020 27th IEEE Int. Conf. on Electronics, Circuits and Systems (ICECS)*, Glasgow, Scotland, UK, IEEE, pp. 1–2, 2020.
- [9] P. Gajbhiye, R. K. Tripathy, A. Bhattacharyya and R. B. Pachori, "Novel approaches for the removal of motion artifact from EEG recordings," *IEEE Sensors Journal*, vol. 19, no. 22, pp. 10600–10608, 2019.
- [10] R. Ranjan, B. C. Sahana and A. K. Bhandari, "Motion artifacts suppression from EEG signals using an adaptive signal denoising method," *IEEE Transactions on Instrumentation and Measurement*, vol. 71, pp. 400–410, 2022.

- [11] Y. E. Lee, N. S. Kwak and S. W. Lee, "A Real-time movement artifact removal method for ambulatory brain-computer interfaces," *IEEE Transactions on Neural Systems and Rehabilitation Engineering*, vol. 28, no. 12, pp. 2660–2670, 2020.
- [12] C. Y. Chang, S. H. Hsu, L. P. Tonachini and T. P. Jung, "Evaluation of artifact subspace reconstruction for automatic artifact components removal in multi-channel EEG recordings," *IEEE Transactions on Biomedical Engineering*, vol. 67, no. 4, pp. 1114–1121, 2019.
- [13] S. Behera and M. N. Mohanty, "Removal of artifact from the brain signal using Discrete Cosine Transform," in *Advances in Electronics, Communication and Computing*, Springer, Singapore, pp. 239–249, 2021.
- [14] S. Behera and M. N. Mohanty, "Template matching based artifact detection from the brain signals," *Online Conference: Michael Faraday IET International Summit: MFIS-2020*, pp. 284–289, 2021.
- [15] Y. Ren, P. N. Suganthan, N. Srikanth and G. Amaratunga, "Random vector functional link network for short-term electricity load demand forecasting," *Information Sciences*, vol. 367, pp. 1078–1093, 2016.
- [16] S. Tong, A. Bezerianos, J. Paul, Y. Zhu and N. Thakor, "Removal of ECG interference from the EEG recordings in small animals using independent component analysis," *Journal of Neuroscience Methods*, vol. 108, no. 1, pp. 11–17, 2001.
- [17] S. Devuyt, T. Dutoit, P. Stenuit, M. Kerkhofs and E. Stanus, "Removal of ECG artifacts from EEG using a modified independent component analysis approach," in *2008 30th Annual Int. Conf. of the IEEE Engineering in Medicine and Biology Society*, Vancouver, BC, Canada, pp. 5204–5207, 2008.
- [18] S. Devuyt, T. Dutoit, P. Stenuit, M. Kerkhofs and E. Stanus, "Cancelling ECG artifacts in EEG using a modified independent component analysis approach," *EURASIP Journal on Advances in Signal Processing*, vol. 2008, no. 1 pp. 1–13, 2008.
- [19] Y. Leclercq, E. Balteau, T. Dang-Vu, M. Schabus, A. Luxen *et al.*, "Rejection of pulse related artefact (PRA) from continuous electroencephalographic (EEG) time series recorded during functional magnetic resonance imaging (fMRI) using constraint independent component analysis (cICA)," *Neuroimage*, vol. 44, no. 3, pp. 679–691, 2009.
- [20] K. Wang, W. Li, L. Dong, L. Zou and C. Wang, "Clustering-constrained ICA for ballistocardiogram artifacts removal in simultaneous EEG-fMRI," *Frontiers in Neuroscience*, 12, vol. 59, pp. 1–13, 2018.
- [21] M. F. Issa, G. Tuboly, G. Kozmann and Z. Juhasz, "Automatic ECG artefact removal from EEG signals." *Measurement Science Review*, vol. 19, no. 3, pp. 101–108, 2019.
- [22] X. R. Zhang, W. F. Zhang, W. Sun, X. M. Sun and S. K. Jha, "A robust 3-D medical watermarking based on wavelet transform for data protection," *Computer Systems Science & Engineering*, vol. 41, no. 3, pp. 1043–1056, 2022.
- [23] M. Marino, Q. Liu, V. Koudelka, C. Porcaro, J. Hlinka *et al.*, "Adaptive optimal basis set for BCG artifact removal in simultaneous EEG-fMRI," *Scientific Reports*, vol. 8, no. 1, pp. 1–11, 2018.
- [24] G. Tamburro, D. B. Stone and S. Comani, "Automatic removal of cardiac interference (ARCI): A new approach for EEG data," *Frontiers in Neuroscience*, vol. 13, pp. 441, 2018.
- [25] C. Dora and P. K. Biswal, "Efficient detection and correction of variable strength ECG artifact from single channel EEG," *Biomedical Signal Processing and Control*, vol. 50, pp. 168–177, 2019.
- [26] S. P. Cho, M. H. Song, Y. C. Park, H. S. Choi and K. J. Lee, "Adaptive noise canceling of electrocardiogram artifacts in single channel electroencephalogram," in *2007 29th Annual Int. Conf. of the IEEE Engineering in Medicine and Biology Society*, Lyon, France, pp. 3278–3281, 2007.
- [27] J. Sijbers, J. V. Audekerke, M. Verhoye, A. V. D. Linden and D. V. Dyck, "Reduction of ECG and gradient related artifacts in simultaneously recorded human EEG/MRI data," *Magnetic Resonance Imaging*, vol. 18, no. 7, pp. 881–886, 2000.
- [28] C. Dai, J. Wang, J. Xie, W. Li, Y. Gong *et al.*, "Removal of ECG artifacts from EEG using an effective recursive least square notch filter," *IEEE Access*, vol. 7, pp. 158872–158880, 2019.
- [29] J. P. Lanquart, M. Dumont and P. Linkowski, "QRS artifact elimination on full night sleep EEG," *Medical Engineering & Physics*, vol. 28, no. 2, pp. 156–165, 2006.
- [30] X. Navarro, F. Porée and G. Carrault, "ECG removal in preterm EEG combining empirical mode decomposition and adaptive filtering," in *2012 IEEE Int. Conf. on Acoustics, Speech and Signal Processing (ICASSP)*, Takaragaike, Sakyo-ku, Kyoto 606-0001 Japan, pp. 661–664, 2012.

- [31] S. S. Priyadharsini and S. E. Rajan, "An efficient method for the removal of ECG artifact from measured EEG signal using PSO algorithm," *International Journal of Advances in Soft Computing Applications*, vol. 6, pp. 1–19, 2016.
- [32] H. N. Suresh and C. Puttamadappa, "Removal of EMG and ECG artifacts from EEG based on real time recurrent learning algorithm," *International Journal of Physical Sciences*, vol. 3, no. 5, pp. 120–125, 2008.
- [33] W. Dai, Q. Chen, F. Chu, X. Ma and T. Chai, "Robust regularized random vector functional link network and its industrial application," *IEEE Access*, vol. 5, pp. 16162–16172, 2017.
- [34] A. Bezerianos, A. S. Tong and N. Thakor, "Time-dependent entropy estimation of EEG rhythm changes following brain ischemia," *Annals of Biomedical Engineering*, vol. 31, no. 2, pp. 221–232, 2003.
- [35] M. A. Klados and P. D. Bamidis, "A Semi-simulated EEG/EOG dataset for the comparison of EOG artifact rejection techniques," *Data in Brief*, vol. 8, pp. 1004–1006, 2016.